Cureus Journal of Engineering

Open Access Original Article

Understanding the Role of Spacers in Modulating Nonlinear Optical Properties of Triphenylamine Derivative Chromophores: A Computational Approach

Review began 12/09/2024
Review ended 12/30/2024
Published 12/31/2024

DOI: https://doi.org/10.7759/s44388-024-02875-4

Balachandar Waddar [1] , Gandi Suman [1] , Saidi R. Parne [1]

1. Department of Applied Sciences, National Institute of Technology Goa, Goa, IND

Corresponding authors: Balachandar Waddar, waddarbalachandra717@gmail.com, Gandi Suman, gandisuman@nitgoa.ac.in, Saidi R. Parne, psreddy@nitgoa.ac.in

Abstract

This study investigates the second-order nonlinear optical (NLO) properties of three novel triphenylamine derivative chromophores: 2,2'-((5-((E)-4-((E)-4-(diphenylamino) styryl) styryl)-1,3-phenylene) bis(methanylylidene)) dimalononitrile abbreviated as S1; 2,2'-((5-((E)-2-(5-((E)-4-(diphenylamino) styryl) furan-2-yl) vinyl)-1,3-phenylene) bis(methanylylidene)) dimalononitrile referred to as S2; and 2,2'-((5-((E)-2-(5-((E)-4-(diphenylamino) styryl)-1H-pyrrol-2-yl) vinyl)-1,3-phenylene) bis(methanylylidene)) dimalononitrile, abbreviated as S3, utilizing density functional theory and time-dependent density functional theory. The study focuses mainly on the impact of two π-spacers, namely furan and pyrrole on the second-order NLO properties of these chromophores. The computational analysis reveals that the pyrrole-substituted chromophore S3 exhibits superior NLO properties, with a dipole moment of 3.78 Debye, linear polarizability of 97.23 × 10^{-24} esu, and first hyperpolarizability of 189455 × 10^{-33} esu. These findings highlight the significance of molecular design in enhancing NLO responses, demonstrating that incorporating strong electron-donating, withdrawing groups, and appropriate π-spacers can improve optical properties. This research contributes to the development of organic NLO materials essential for various photonic applications, including optical communication and other potential uses.

Categories: Advanced Materials
Keywords: organic nlo materials, nonlinear optics, spacer effects, triphenylamine derivative, dft

Introduction

Organic molecules are crucial in the development of nonlinear optical (NLO) technologies due to their distinct advantages over conventional inorganic and complex materials. These advantages include molecular tailoring, high NLO responses, a broad range of structural possibilities, self-assembly, lower dielectric constants, and high damage thresholds, which collectively make organic molecules essential for technologies such as optical switches used in telecommunications for fast data processing, sensors, and frequency converters used in applications of medicine, sensing, and spectroscopy, quantum computing, and material processing, etc. [1-8]. These advancements drive innovation in imaging, telecommunications, and various other fields. Over the past three decades, a variety of organic materials have been engineered for second-order nonlinear applications to enhance their first hyperpolarizability [9]. This first hyperpolarizability is a key consideration for second-order NLO materials, functioning as a guiding parameter in the design and application of organic materials in photonics, and is closely linked to the strength of the nonlinear response.

Typical NLO materials are of a push-pull type with a π-conjugated system and D-π-A type organic chromophores demonstrating enhanced NLO properties [10-12]. In this context, the π represents a conjugated bridge formed by π-π* bonds that facilitate charge transfer and enhance NLO activity, while D and A denote the donor and acceptors, respectively, which are responsible for donating and withdrawing electrons.

Numerous studies on organic molecules have demonstrated the feasibility of modifying their optical, electrical, and chemical properties by varying the donor, acceptor, and π spacers, and also significant changes will be observed in the NLO properties of the molecules. These π spacers are particularly noteworthy due to their ability to enhance electron delocalization, modify optical features, improve nonlinear responses, and influence molecular interactions. Notable examples of such π spacers include furan, thiophane, and pyrrole, which have been highlighted in the literature [13-15] for their unique electronic properties, stability, versatility, and electron-rich nature, all of which significantly contribute to the delocalization of electrons. Furan is a five-membered aromatic heterocyclic compound with a planar structure, has shown considerable stability and is widely utilized in various NLO applications. Similarly, pyrrole-based compounds exhibit strong NLO properties due to their electron-rich nature and extended conjugation, making them potential candidates for these applications. Recent studies have also garnered

How to cite this article
Waddar B, Suman G, Parne S R (December 31, 2024) Understanding the Role of Spacers in Modulating Nonlinear Optical Properties of Triphenylamine Derivative Chromophores: A Computational Approach. Cureus J Eng 1 : es44388-024-02875-4. DOI https://doi.org/10.7759/s44388-024-02875-4

interest in triphenylamine derivatives; triphenylamine acts as an efficient electron donor in organic materials due to its electron-rich nitrogen, its nitrogen lone pair with the π-electrons of the phenyl rings, leading to delocalized electronic states that facilitate charge transfer atom and conjugated structure [16], which have applications in diverse fields such as dye-sensitized solar cells, optoelectronics, and medicinal chemistry, indicating promising candidates. Consequently, triphenylamine, used as the donor in this study, has played a significant role in these chromophores, while nitro groups serve as acceptors [17]. In designing materials and assessing their potential electrical, optical, and NLO properties, the density functional theory (DFT) approach offers several advantages. In this study, we report on three novel triphenylamine derivative chromophores (Figure *1*), with triphenylamine 2,2'-((5-((E)-4-((E)-4-(diphenylamino) styryl) styryl)-1,3-phenylene) bis(methanylylidene)) dimalononitrile abbreviated as S1, serving as a reference for evaluating the impact of two π-spacers, furan substituted 2,2'-((5-((E)-2-(5-((E)-4-(diphenylamino) styryl) furan-2-yl) vinyl)-1,3-phenylene) bis(methanylylidene)) dimalononitrile, abbreviated as S2, and pyrrole-substituted 2,2'-((5-((E)-2-(5-((E)-4-(diphenylamino) styryl)-1H-pyrrol-2-yl) vinyl)-1,3-phenylene) bis(methanylylidene)) dimalononitrile, abbreviated as S3, and estimate their second-order nonlinear optical properties by using density functional theory.

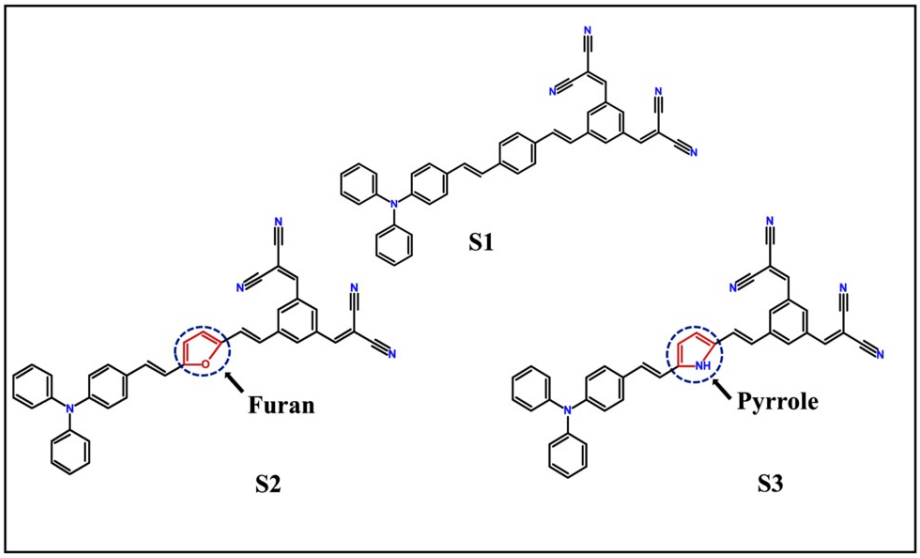

FIGURE 1: Triphenylamine derivative chromophores

Materials And Methods

In this study, all calculations were carried out on the DFT platform, using Gaussian 16 program package for both ground and excited state calculations in the gaseous phase [18]. All three chromophores, S1, S2, and S3, belong to C1 point group symmetry. Initially, geometry optimization of each molecule in the ground state was performed using the 6-311++G(d,p) basis set with the ωB97XD functional [19,20]. This functional was chosen for its accuracy, efficiency, and capability to effectively address long-range interactions and dispersion effects. No negative frequencies were observed in the optimized structures, which were subsequently used to calculate NLO and related properties. Time-dependent DFT (TD-DFT) is known as a robust and reliable method for calculating UV-visible spectra, yielding valuable insights into the electronic properties of the molecules. It was employed to obtain the oscillator strength, along with the UV-visible spectra.

Results

Dipole moment

The dipole moment (μ) is a crucial parameter in the NLO studies of organic molecules, as it affects their susceptibility, polarizability, charge transfer, and overall molecular interactions. The dipole moment is influenced by various factors, including the molecular geometry, electronegativity of the atoms, functional groups, and the π-conjugated system within the molecule [21]. For the S1, S2, and S3 chromophores, the dipole moment values were determined using the ωB97XD/6-311++G(d,p) method in the ground state. The net dipole moment (μ) was then calculated using Equation (1), with the results presented in Table *1*.

$$\text{Dipole moment} \quad \mu = \left(\mu_x^2 + \mu_y^2 + \mu_z^2\right)^{1/2} \text{ in Debye} \qquad (1)$$

Table *1* indicates the calculated net dipole moment (μ) for all designed chromophores found in the range of 3.34 to 3.78 Debye. Among the three chromophores, the pyrrole-substituted chromophore S3 displays the

highest dipole moment. This increase is attributed to the presence of electronegative atoms, which contribute to a greater extent of partial charges compared to the other molecules.

Chromophore	Dipole moment (in Debye)	Linear polarizability (in 10^{-24} esu)	First hyperpolarizability (in 10^{-33} esu)
S1	3.34	96.57	170412
S2	3.74	94.68	174063
S3	3.78	97.23	189455

TABLE 1: Dipole moment (μ) (in Debye), linear polarizability (α) (in 10-24 esu) and first hyperpolarizability (β) (in 10-34 esu), calculated at ωB97XD/ 6311++G (d,p) level

Linear polarizability

Linear polarizability (α) is an important property in organic NLO materials, as it influences both linear and NLO responses. It quantifies the distortion of a molecule's electron cloud when subjected to an applied electric field, which directly impacts the optical properties of the materials [22]. Organic materials that feature conjugated systems with delocalized π-electron configurations typically exhibit large linear polarizabilities. Enhancements in polarizability can result from factors such as molecular structure, electron delocalization, and functional group substitution, making it a critical consideration in the design of materials with improved NLO properties. The average linear polarizability (α) for the chromophores S1, S2, and S3 was calculated using the ωB97XD/6-311++G(d,p) method in the ground state, and the average values were obtained using Equation (2).

$$\alpha = \frac{1}{3}\left(\alpha_{xx} + \alpha_{yy} + \alpha_{zz}\right) \text{ esu} \qquad (2)$$

Table *1* presents the α values for the chromophores S1, S2, and S3. Notably, the α value for S2 is 97.23 × 10^{-24} esu in the gaseous phase, representing the highest value among the three chromophores and indicating its highly polarizable nature. In comparison, while the chromophores exhibit comparable α values overall, the trend observed in their polarizability is S1 > S2 > S3.

First hyperpolarizability

The first hyperpolarizability (β) is crucial for determining the efficacy of second-order NLO effects [23]. It is influenced by various factors, including molecular conjugation, the presence of electron-donating or withdrawing groups, molecular symmetry, size, charge transfer properties, and solvent effects. Expressed as a 3 × 3 × 3 matrix, the first hyperpolarizability is categorized as a third-rank tensor. Through the application of Kleinman symmetry, this matrix is reduced from its original 27 components to 10. In this study, the static first hyperpolarizability of the S1, S2, and S3 chromophores was obtained using the ωB97XD/6-311++G(d,p) method in the gaseous phase, with further calculations performed using Equation (3) to assess their NLO activity. The results are presented in Table *1*.

$$(\beta_{\text{total}} = \left[\left(\beta_{xxx} + \beta_{xyy} + \beta_{xzz}\right)^2 + \left(\beta_{yyy} + \beta_{xxy} + \beta_{yyz}\right)^2 + \left(\beta_{zzz} + \beta_{xxz} + \beta_{yyz}\right)^2\right]^{1/2}$$

(3)

Table *1* reveals that the values of the first hyperpolarizability (β) follow the order S1 > S2 > S3, clearly indicating that the pyrrole-substituted chromophore S3 exhibits higher values. This enhancement is attributed to the presence of lone pairs of electrons and greater electron delocalization compared to the other two chromophores.

Frontier molecular orbitals

Frontier molecular orbitals (FMOs) are commonly referred as the Highest Occupied Molecular Orbital (HOMO) and the Lowest Unoccupied Molecular Orbital (LUMO). The energy gap between these two orbitals significantly influences a material's electronic charge properties and its NLO performance. The values of HOMO and LUMO, presented in Table *2* and Figure *2*, were obtained using the ωB97XD/6-311++G(d,p) method in the gaseous phase. A small HOMO-LUMO gap indicates that electrons can transition from the HOMO to the LUMO with relative ease and minimal energy required, which typically signifies higher reactivity [24,25].

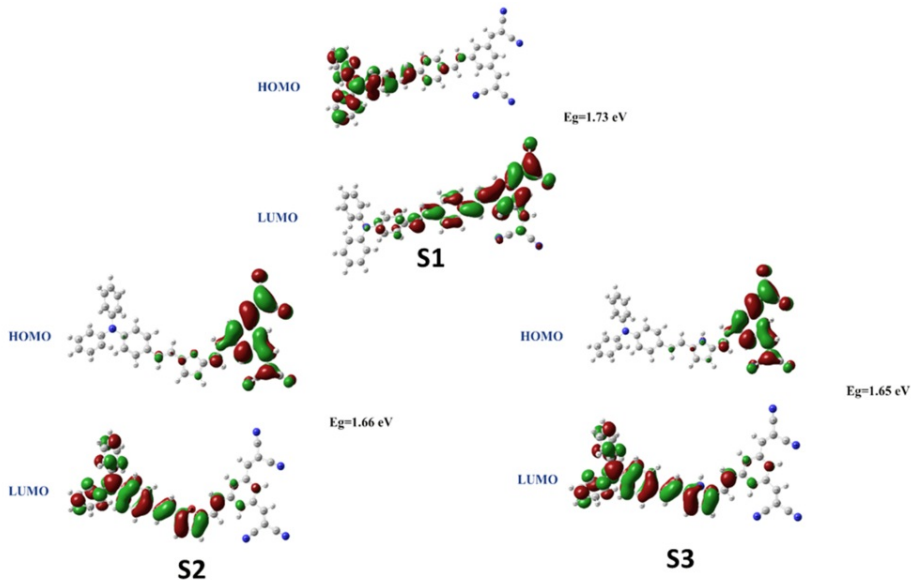

FIGURE 2: HOMO LUMO of chromophores S1, S2, and S3

HOMO, Highest Occupied Molecular Orbital; LUMO, Lowest Unoccupied Molecular Orbital

Chemical hardness (η) and softness (σ) are critical factors influencing a molecule's stability and reactivity, especially in the realm of organic NLO materials [26-28]. Chemical hardness represents the resistance to electron flow, indicating a material's stability and lower reactivity. In contrast, softness refers to a material's tendency to donate electrons, enhancing both its reactivity and polarizability. Generally, materials characterized by lower hardness or higher softness tend to exhibit stronger NLO properties, as they can readily undergo electron transitions, which are essential for NLO applications. Soft materials are particularly efficient in processes like second-harmonic generation and optical switching. Therefore, optimizing both hardness and softness is crucial for the design of effective organic NLO materials. The calculations for chemical hardness and softness are provided using Equations (4) and (5), with the results displayed in Table *2*. These values indicate a very narrow HOMO-LUMO gap, suggesting that the materials are soft and highly reactive.

$$\eta = \frac{1}{2}\left(E_{\mathrm{LUMO}} - E_{\mathrm{HOMO}}\right) \quad (4)$$

$$\sigma = \frac{1}{\eta} \quad (5)$$

Chromophore	HOMO (in eV)	LUMO (in eV)	Energy gap (in eV)	Chemical softness	Chemical hardness
S1	−7.85	−6.12	1.73	0.865	1.156
S2	−7.74	−6.08	1.66	0.83	1.204
S3	−7.72	−6.07	1.65	0.825	1.212

TABLE 2: Chemical hardness (η) (in eV), chemical softness (σ) (in eV), HOMO, and LUMO (in au) for π→π* interactions calculated at ωB3LYP/6–311+ +G (d,p)

HOMO, Highest Occupied Molecular Orbital; LUMO, Lowest Unoccupied Molecular Orbital

Molecular electrostatic potential

The molecular electrostatic potential (MEP) significantly simplifies the process of identifying the relative reactivity locations within molecules for both nucleophilic and electrophilic interactions [29]. In this study, the MEP surface for the chromophore S1 was determined using the optimized structure obtained from the ωB97XD/6-311++G(d,p) method. The electrostatic potential surface of the molecule is depicted in Figure *3*,

with a color code that ranges from −5.836e−2 to +5.836e−2. A red-blue gradient is employed to differentiate areas rich in electrons from those deficient in them. The red regions, which represent negative potential, are localized over the nitro groups, indicating that these sites are likely targets for nucleophilic attacks. Conversely, the blue regions signify positive potential, concentrated around the nitro groups, suggesting that these regions may serve as donors and are likely the primary sites for electrophilic interactions. Thus, understanding the reactivity and interactions within the molecule relies on the careful identification of electron-rich and electron-deficient regions through MEP analysis.

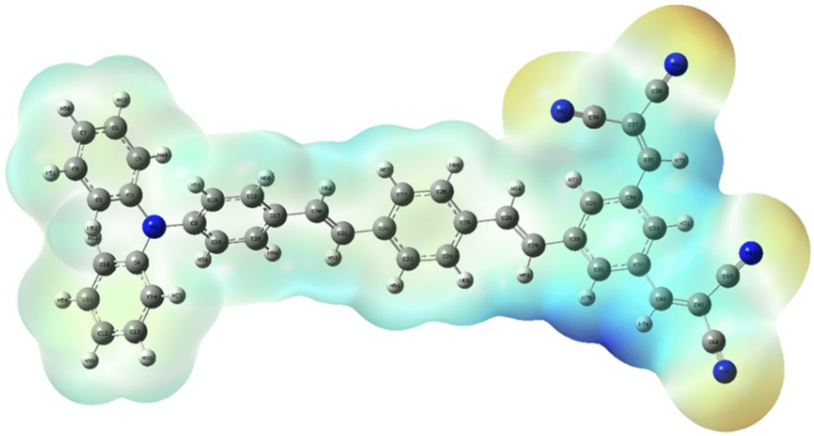

FIGURE 3: Electrostatic potential surface of S1

Natural bond orbital (NBO) analysis

NBO analysis plays a crucial role in understanding and enhancing charge transfer, electron delocalization, and molecular orbital interactions, all of which are essential for improving the NLO characteristics of materials. As NBO is an important computational tool, the analysis focuses on examining the bonding, antibonding, and charge transfer mechanisms. NBO theory interprets electronic wave functions as a collection of unoccupied non-Lewis orbitals, such as anti-bonding or Rydberg states, alongside occupied Lewis-type orbitals, including bonding and lone pairs [30-32]. Table *3* outlines the interactions between the unoccupied non-Lewis NBOs and occupied Lewis-type NBOs, with calculations performed in the gaseous phase using the ωB97XD/6-311++G(d,p) method. This table highlights stabilizing donor-acceptor interactions and provides a comprehensive overview of electron density delocalization (Figure *4*). The stabilization energies of all possible interactions between donor and acceptor orbitals within the NBO framework can be evaluated using second-order perturbation theory. The application of second-order perturbation theory in this context allows for the determination of stabilization energy, as described by Equation (6).

$$E^{(2)} = q_i \frac{F^2(i,j)}{\epsilon_j - \epsilon_i} \qquad (6)$$

Where F^2 (i,j) represents the off-diagonal matrix elements, qi gives the occupancy of the donor orbitals, εj and εi give the values of the donor and acceptor orbital energies, and E(2) computes the interaction's magnitude using the donor and acceptor orbitals. Electronic transitions can be categorized into several types, with four typical kinds being recognized: σ→σ*, π→π*, LP→σ*, and LP→π*. Among these, the π→π* transitions are the most significant. Table *3* highlights a few possible and important electronic transitions between Lewis-type NBOs to non-Lewis-type NBOs of chromophore S1, specifically from C34-C35 to C36-C37, C34-C35 to C36-C37, C2-C19 to C15-C16, N1 to C2-C19, and N46 to C28-C29. These transitions are considered particularly important, with corresponding energy values of 572.70, 1.62, 28.92, 29.87, and 32.53 kJ/mol, respectively. This implies that the strongest interaction is C34-C35 to C36-C37, N1 to C2-C19, and C34-C35 to C36-C37 being the weakest interaction. It confirms that π-π* type interaction will play a significant role in electron delocalization and intramolecular charge transfer, resulting in a significant first hyperpolarizability value.

Donor (i)	Type	ED(e)	Acceptor (j)	Type	ED(e)	E(2) a(kJ/mol)	E(j)-E(i)	F(i,j)
N1	σ	1.73995	C2-C19	π*	0.38710	29.87	0.39	0.099

N45	σ	1.97069	C28-C29	σ^*	0.01415	3.95	0.33	0.033
N46	σ	1.97204	C28-C29	σ^*	0.01415	32.53	0.33	0.093
N47	σ	1.97114	C28-C29	σ^*	0.01415	4.00	0.34	0.033
N1-C2	σ	1.98024	N1-C4	σ^*	0.03785	2.39	1.37	0.051
N1-C3	σ	1.97944	N1-C2	σ^*	0.03790	2.40	1.37	0.051
N1-C4	σ	1.97950	N1-C2	σ^*	0.03790	2.38	1.37	0.051
C2-C15	σ	1.96654	C2-C19	σ^*	0.38710	4.26	1.44	0.070
C2-C19	σ	1.97326	C2-C15	σ^*	0.02443	4.38	1.42	0.071
C2-C19	π	1.64688	C15-C16	π^*	0.30623	28.92	0.40	0.097
C2-C19	π	1.64688	C17-C18	π^*	0.38207	35.65	0.39	0.106
C3-C5	σ	1.97106	C3-C9	σ^*	0.02608	4.47	1.45	0.072
C3-C9	π	1.65238	C7-C8	π^*	0.34271	40.72	0.36	0.108
C4-C14	π	1.65247	C12-C13	π^*	0.34423	37.01	0.40	0.108
C5-C6	π	1.67720	C7-C8	π^*	0.34271	36.02	0.35	0.101
C7-C8	π	1.66581	C5-C6	π^*	0.33138	37.22	0.39	0.108
C10-C11	π	1.67578	C4-C14	π^*	0.38261	35.79	0.39	0.107
C12-C13	π	1.66585	C10-C11	π^*	0.33080	37.83	0.39	0.108
C15-C16	σ	1.97203	C16-C17	σ^*	0.02746	4.52	1.37	0.070
C15-C16	π	1.69652	C17-C18	π^*	0.38207	30.09	0.39	0.099
C17-C18	π	1.63286	C20-C21	π^*	0.11521	19.05	0.42	0.085
C20-C21	π	1.88696	C22-C27	π^*	0.36778	15.44	0.42	0.077
C21-C22	σ	1.97347	C43-N47	σ^*	0.01040	409.23	0.02	0.083
C23-C24	π	1.68505	C22-C27	π^*	0.36778	33.69	0.39	0.104
C24-C25	σ	1.97164	C23-C24	σ^*	0.01431	3.71	1.45	0.066
C25-C26	π	1.62228	C22-C27	π^*	0.36778	34.42	0.38	0.102
C26-C27	σ	1.97616	C25-C28	σ^*	0.02421	4.20	1.27	0.065
C28-C29	σ	1.97596	C42-N46	δ^*	0.06748	225.96	0.02	0.056
C29-C30	σ	1.97292	C30-C31	σ^*	0.02161	7.53	1.35	0.090
C30-C31	σ	1.97293	C32-C33	σ^*	0.02568	4.80	1.20	0.068
C31-C32	σ	1.97326	C32-C40	σ^*	0.02251	11.54	1.36	0.112
C32-C33	σ	1.97263	C34-C36	σ^*	0.02292	21.73	6.05	0.324
C32-C33	π	1.61956	C30-C31	π^*	0.33223	32.87	0.40	0.103
C34-C35	σ	1.97230	C36-C37	σ^*	0.02137	1.62	3.32	0.066
C34-C35	π	1.61102	C36-C37	π^*	0.14873	572.70	0.22	0.325
C36-C37	σ	1.96943	C39-N45	σ^*	0.01020	359.67	0.57	0.407

C37-C39	σ	1.97383	C38-N44	δ^*	0.06401	748.29	0.05	0.167
C41-C42	σ	1.96714	C17-C18	σ^*	0.02090	14748.85	0.02	0.425
C41-C43	σ	1.96879	C17-C18	σ^*	0.02090	3269.10	0.01	0.186
C42-N46	π	1.98495	C28-C29	σ^*	0.01415	165.99	0.18	0.153
C43-N47	σ	1.99355	C42-N46	δ^*	0.06748	95.07	0.37	0.170

TABLE 3: NBO analysis calculated at ωB97XD 6311++G (d,p) level

NBO, natural bond orbital

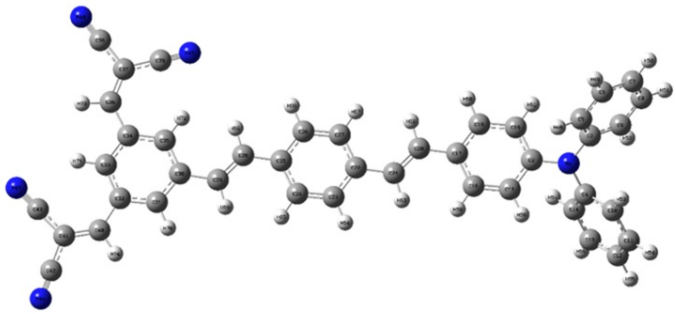

FIGURE 4: Schematic representation of charge flow in molecule S1

Discussion

UV-visible spectra

The UV-visible spectra are crucial for understanding the electronic structure, absorption characteristics, and excited-state electronic transitions in NLO materials [33]. Oscillator strength is critical as it specifies the intensity of each electronic transition and correlates with the material's ability to absorb light, which directly affects its NLO optical behavior. High oscillator strengths are correlated with strong transitions, while low oscillator strengths are linked to weak transitions.

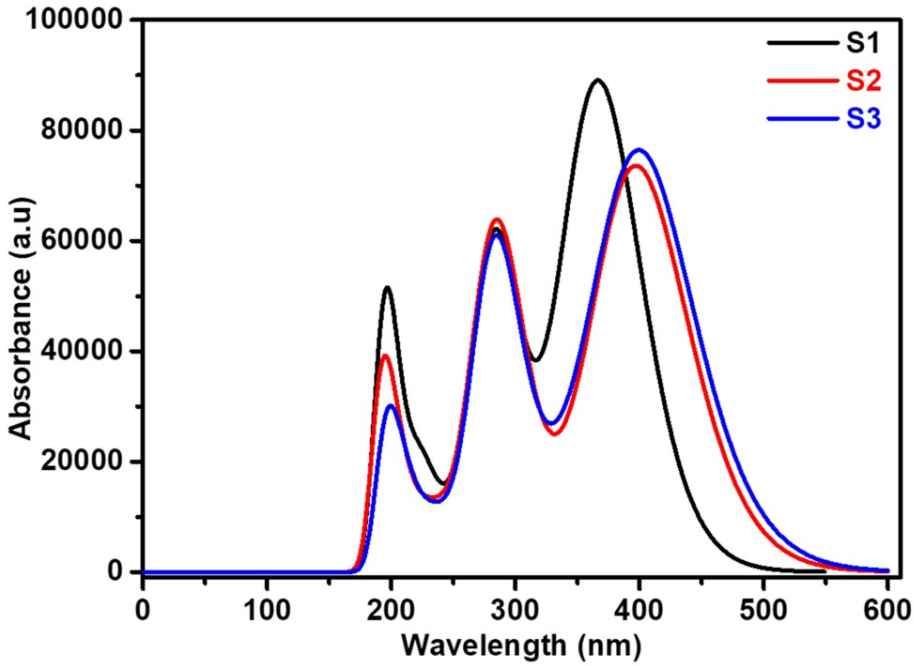

FIGURE 5: UV-visible spectrum of TM1 recorded at ωB97XD/6-311++G(d,p) with n = 50 (n is the number of excited states and the wavelength in nm)

UV-visible spectra for the chromophores S1, S2, and S3 were obtained through TD-DFT calculations using the ωB97XD/6-311++G(d,p) method. The resultant UV-visible spectra, illustrated in Figure *5*, show absorption bands for chromophores S1, S2, and S3 at 373.93 nm, 409.58 nm, and 397.17 nm, respectively, as detailed in Table *4*. These absorption bands are primarily attributed to electron transitions involving n and π bonds, as well as nonbonding electrons. Typically, such absorptions result from electron transitions related to lone pairs or conjugated systems within the molecules. Notably, the oxygen atom in furan is more electronegative than the nitrogen atom in pyrrole, leading to furan absorbing at a longer wavelength than pyrrole. This characteristic results in a wider HOMO-LUMO gap for furan, which in turn corresponds to lower energy absorption.

Compound	S1	S2	S3
Wavelength (nm)	373.93	409.58	397.17
Oscillator strength	1.2874	0.9268	1.4472

TABLE 4: UV-visible spectrum, oscillator strength recorded at ωB97XD/6-311++G(d,p) with n = 60 (n is the number of excited states)

Conclusions

This study focused on the second-order NLO properties of three distinct triphenylamine derivative chromophores substituted with two π spacers. The results indicated that when strong electron-donating groups were substituted with spacers S2 and S3, these molecules exhibited significantly higher dipole moments and first hyperpolarizability values. Specifically, S3 demonstrated a first hyperpolarizability (β) of 189,455.202 × 10^{-34} esu, a dipole moment (μ) of 3.78 Debye, and a polarizability (α) of 97.23 × 10^{-24} esu, determined using the ωB97XD functional with a 6-311++G(d,p) basis set. Additionally, S3 presented a low energy band gap of 1.65 eV, with NBO analysis confirming the highest charge transfer capacity among the three derivatives. These molecules also exhibited strong absorption maxima in the ultraviolet region, which, along with their lower HOMO-LUMO energy gap stemming from their aromatic structure, suggests favorable conditions for NLO applications. Furthermore, the derivatives displayed good thermal stability, indicating that structural tailoring with various electron-rich donor substituents could enhance the NLO response. Their promising candidacy for NLO applications is further supported by the observed smaller energy gap,

suggesting potential for intermolecular charge transfer within the π-conjugated molecular system.

Additional Information

Author Contributions

All authors have reviewed the final version to be published and agreed to be accountable for all aspects of the work.

Concept and design: Saidi R. Parne, Balachandar Waddar

Critical review of the manuscript for important intellectual content: Saidi R. Parne, Gandi Suman

Supervision: Saidi R. Parne

Acquisition, analysis, or interpretation of data: Gandi Suman, Balachandar Waddar

Drafting of the manuscript: Balachandar Waddar

Disclosures

Human subjects: All authors have confirmed that this study did not involve human participants or tissue. **Animal subjects:** All authors have confirmed that this study did not involve animal subjects or tissue. **Conflicts of interest:** In compliance with the ICMJE uniform disclosure form, all authors declare the following: **Payment/services info:** All authors have declared that no financial support was received from any organization for the submitted work. **Financial relationships:** All authors have declared that they have no financial relationships at present or within the previous three years with any organizations that might have an interest in the submitted work. **Other relationships:** Dr. Parne is an associate editor at the Cureus Journal of Engineering.

Acknowledgements

The authors gratefully thank Professor Jens Dittmer for the provision of computational cluster facility “Simulation Numerique” at the Institut des Molécules et Matériaux du Mans, Le Mans Université, Le Mans, France.

References

1. Basu S: A review of nonlinear optical organic materials . Industrial & Engineering Chemistry Product Research and Development. 1984, 23:183-86. 10.1021/i300014a001
2. Waddar B, Parne SR, Gandi S, Prasanth GR, Yaseen M, Karidurаganavar MY: The second-order nonlinear optical properties of novel triazolo[3,4-b] [1, 3, 4] thiadiazole derivative chromophores using DFT calculations. Structural Chemistry. 2023, 35:253-64. 10.1007/s11224-023-02178-0
3. Waddar B, Gandi S, Parne SR, Chari VR, Prasanth GR: Investigation of second-order NLO properties of novel 1,3,4-oxadiazole derivatives: a DFT study. Journal of Molecular Modeling. 2024, 30:1-14. 10.1007/s00894-024-05910-7
4. Karidurаganavar MY, Doddamani RV, Waddar B, Parne SR: Nonlinear optical responsive molecular switches . Nonlinear Optics-From Solitons to Similaritons. Nalan Antar, İlkay Bakırtaş (ed): IntechOpen, 2021. 187. 10.5772/intechopen.92675
5. Liu J, Ouyang C, Huo F, He W, Cao A: Progress in the enhancement of electro-optic coefficients and orientation stability for organic second-order nonlinear optical materials. Dyes and Pigments. 2020, 181:108509. 10.1016/j.dyepig.2020.108509
6. Jazbinsek M, Puc U, Abina A, Zidansek A: Organic crystals for THz photonics . Applied Sciences. 2019, 9:882. 10.3390/app9050882
7. Nicoletti D, Cavalleri A: Nonlinear light-matter interaction at terahertz frequencies . Advances in Optics and Photonics. 2016, 8:401-64. 10.1364/aop.8.000401
8. Hirori H, Doi A, Blanchard F, Tanaka K: Single-cycle terahertz pulses with amplitudes exceeding 1 MV/cm generated by optical rectification in LiNbO3. Applied Physics Letters. 2011, 98: 091106. 10.1063/1.3560062
9. Yoshioka K, Minami Y, Shudo KI, et al.: Terahertz-field-induced nonlinear electron delocalization in Au nanostructures. Nano Letters. 2015, 15:1036-40. 10.1021/nl503916t
10. Marder SR, Perry JW, Tiemann BG, Marsh RE, Schaefer WP: Second-order optical nonlinearities and photostabilities of 2-N-methylstilbazolium salts. Chemistry of Materials. 1990, 2:685-90. 10.1021/cm00012a017
11. Azaid A, Alaqarbeh M, Abram T, et al.: D-π-A push-pull chromophores based on N,N-Diethylaniline as a donor for NLO applications: effects of structural modification of π-linkers. Journal of Molecular Structure. 2024, 1295:136602. 10.1016/j.molstruc.2023.136602
12. Kim TD, Lee KS: D-π-A conjugated molecules for optoelectronic applications. Macromolecular Rapid Communications. 2015, 36:943-58. 10.1002/marc.201400749
13. Nieman R, Tsai H, Nie W, et al.: The crucial role of a spacer material on the efficiency of charge transfer processes in organic donor-acceptor junction solar cells. Nanoscale. 2017, 10:451-59. 10.1039/c7nr07125f
14. Yang J, Guo F, Hua J, Li X, Wu W, Qua Y, Tian H: Efficient and stable organic DSSC sensitizers bearing

quinacridone and furan moieties as a planar π-spacer. Journal of Materials Chemistry. 2012, 22:24356-65. 10.1039/c2jm31929b

15. Jia J, Chen Y, Duan L, Sun Z, Liang M, Xue S: New D-π-A dyes incorporating dithieno[3,2-b:2′,3′-d]pyrrole (DTP)-based π-spacers for efficient dye-sensitized solar cells. RSC Advances. 2017, 7:45807-817. 10.1039/c7ra08965a
16. Mahmood A, Khan SUD, Rana UA, et al.: Effect of thiophene rings on UV/visible spectra and non-linear optical (NLO) properties of triphenylamine based dyes: a quantum chemical perspective. Journal of Physical Organic Chemistry. 2015, 28:418-22. 10.1002/poc.3427
17. Xu J: Synthesis of β-lactams with π electron-withdrawing substituents . Tetrahedron. 2012, 68:10696-747. 10.1016/j.tet.2012.04.007
18. Vennila M, Rathikha R, Muthu S, Jeelani A, Irfan A: Theoretical structural analysis (FT-IR, FT-R), solvent effect on electronic parameters NLO, FMO, NBO, MEP, UV (IEFPCM model), Fukui function evaluation with pharmacological analysis on methyl nicotinate. Computational and Theoretical Chemistry. 2022, 1217:113890. 10.1016/j.comptc.2022.113890
19. Chai JD, Head-Gordon M: Systematic optimization of long-range corrected hybrid density functionals . The Journal of Chemical Physics. 2008, 128:084106. 10.1063/1.2834918
20. Chai JD, Head-Gordon M: Long-range corrected hybrid density functionals with damped atom-atom dispersion corrections. Physical Chemistry Chemical Physics. 2008, 10:6615-20. 10.1039/b810189b
21. Jiang X, Zhao S, Lin Z, Luo J, Bristowe PD, Guan X, Chen C: The role of dipole moment in determining the nonlinear optical behavior of materials: ab initio studies on quaternary molybdenum tellurite crystals. Journal of Materials Chemistry C. 2014, 2:530-37. 10.1039/c3tc31872a
22. Ahn M, Kim MJ, Cho DW, Wee KR: Electron push-pull effects on intramolecular charge transfer in perylene-based donor-acceptor compounds. The Journal of Organic Chemistry. 2020, 86:403-13. 10.1021/acs.joc.0c02149
23. Acemioğlu B, Arık M, Efeoğlu H, Onganer Y: Solvent effect on the ground and excited state dipole moments of fluorescein. Journal of Molecular Structure THEOCHEM. 2001, 548:165-71. 10.1016/s0166-1280(01)00513-9
24. Parthasarathy V, Pandey R, Das PK, Castet F, Blanchard-Desce M: Linear and nonlinear optical properties of tricyanopropylidene-based merocyanine dyes: synergistic experimental and theoretical investigations. ChemPhysChem. 2018, 19:187-97. 10.1002/cphc.201701143
25. Drissi M, Benhalima N, Megrouss Y, Rachida R, Chouaih A, Hamzaoui F: Theoretical and experimental electrostatic potential around the m-nitrophenol molecule. Molecules. 2015, 20:4042-54. 10.3390/molecules20034042
26. Shimizu A, Ishizaki Y, Horiuchi S, Hirose T, Matsuda K, Sato H, Yoshida JI: HOMO-LUMO energy-gap tuning of π-conjugated zwitterions composed of electron-donating anion and electron-accepting cation. The Journal of Organic Chemistry. 2021, 86:770-81. 10.1021/acs.joc.0c02343
27. Kaya S, Kaya C: A new method for calculation of molecular hardness: a theoretical study . Computational and Theoretical Chemistry. 2015, 1060:66-70. 10.1016/j.comptc.2015.03.004
28. Pearson RG: Hard and soft acids and bases—the evolution of a chemical concept . Coordination Chemistry Reviews. 1990, 100:403-25. 10.1016/0010-8545(90)85016-l
29. Suvitha A, Venkataramanan N, Sahara R, Kawazoe Y: A theoretical exploration of the intermolecular interactions between resveratrol and water: a DFT and AIM analysis. Journal of Molecular Modeling. 2019, 25:1-11. 10.1007/s00894-019-3941-7
30. Demircioğlu Z, Kaştaş ÇA, Büyükgüngör O: Theoretical analysis (NBO, NPA, Mulliken Population Method) and molecular orbital studies (hardness, chemical potential, electrophilicity and Fukui function analysis) of (E)-2-((4-hydroxy-2-methylphenylimino)methyl)-3-methoxyphenol. Journal of Molecular Structure. 2015, 1091:183-95. 10.1016/j.molstruc.2015.02.076
31. Sheela N, Muthu S, Sampathkrishnan S: Molecular orbital studies (hardness, chemical potential and electrophilicity), vibrational investigation and theoretical NBO analysis of 4-4′-(1H-1,2,4-triazol-1-yl methylene) dibenzonitrile based on abinitio and DFT methods. Spectrochimica Acta Part A: Molecular and Biomolecular Spectroscopy. 2014, 120:237-51. 10.1016/j.saa.2013.10.007
32. Rizwana BF, Prasana JC, Muthu S, Abraham CS: Spectroscopic (FT-IR, FT-Raman, NMR) investigation on 2-[(2-amino-6-oxo-6,9-dihydro-3H-purin-9-yl)methoxy]ethyl(2S)-2-amino-3-methylbutanoate by Density Functional Theory. Materials Today: Proceedings. 2019, 18:1770-82. 10.1016/j.matpr.2019.05.276
33. Gelfand N, Freidzon A, Vovna V: Theoretical insights into UV-Vis absorption spectra of difluoroboron β-diketonates with an extended π system: an analysis based on DFT and TD-DFT calculations. Spectrochimica Acta Part A: Molecular and Biomolecular Spectroscopy. 2019, 216:161-72. 10.1016/j.saa.2019.02.064